All-Fullerene-Based Cells for Nonaqueous Redox Flow Batteries

Jochen Friedl,[†] Maria A. Lebedeva,[‡] Kyriakos Porfyrakis,[‡] Ulrich Stimming,*[,†] and Thomas W. Chamberlain*[,§]

[†]Chemistry - School of Natural and Environmental Sciences, Newcastle University, Bedson Building, Newcastle upon Tyne, NE1 7RU, U.K.

[‡]Department of Materials, University of Oxford, 16 Parks Road, Oxford, OX1 3PH, U.K.

[§]Institute of Process Research and Development, School of Chemistry, University of Leeds, Leeds, LS2 9JT, U.K.

S *Supporting Information*

ABSTRACT: Redox flow batteries have the potential to revolutionize our use of intermittent sustainable energy sources such as solar and wind power by storing the energy in liquid electrolytes. Our concept study utilizes a novel electrolyte system, exploiting derivatized fullerenes as both anolyte and catholyte species in a series of battery cells, including a symmetric, single species system which alleviates the common problem of membrane crossover. The prototype multielectron system, utilizing molecular based charge carriers, made from inexpensive, abundant, and sustainable materials, principally, C and Fe, demonstrates remarkable current and energy densities and promising long-term cycling stability.
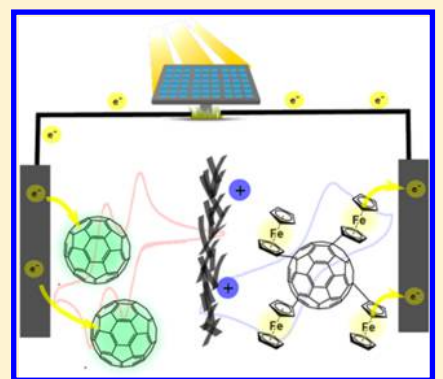
INTRODUCTION

Redox flow batteries (RFBs) represent an exciting opportunity to tackle the problem of energy storage, offering the potential of large scale, affordable, and safe systems. Generally external energy is utilized to drive the cell reaction in a thermodynamically uphill direction, by generating oxidized species at the cathode and reduced species at the anode, after which the species are flowed into a tank and stored until the energy is required. To release the stored energy the system is discharged by flowing species back into the cell to react at the electrodes. The efficiency of this process depends on several factors including the following: the concentration of reactive species in the solutions, the formal potential of the redox couples, the kinetics of the electrochemical processes, and the stability of the active species. Moreover, it is important to consider the safety and cost of the active materials if scale-up is going to be viable.[1] A number of candidate materials have been proposed and explored as redox species in recent years including aqueous systems with all-vanadium (VRB), iron−chromium, polysulfide−bromine redox couples.[2] Such systems, though effective, generally suffer from low power- and energy-density and, in the case of the all-vanadium system, high overall costs due to the expensive active species.

Recently, a number of novel chemistries have been proposed that utilize organic redox electrolytes prepared from inexpensive precursors. For example, in aqueous solvents hydroxylated anthraquinones (AQDS),[3,4] hexacyanoferrate,[4] viologen and ferrocene,[5] and redox-active polymers[6] were reported. Nonaqueous chemistries employing phenothiazine derivates,[7] benzothiadiazole,[8] 2,5-di*tert*-butyl-1-methoxy-4-[2-methoxyethoxy]benzene as the catholyte with 9-fluorenone[9] or *N*-methylphtalimide[10] (NMP) as the anolyte have been reported with high solubility (>0.3 M) of the redox species. For recent reviews on chemistries for RFBs, see refs 11−13. While these systems propose avenues to reach the Advanced Projects Research Agency-Energy (ARPA-e) defined goal of $100 kW h^{-1}, none of the reported systems are able to emulate the biggest advantage of the VRB: Usage of an electrolyte with a single redox active molecule which remedies irreversible capacity loss due to crossover through the membrane.

Fullerene derivatives have the capacity to accept multiple electrons, undergo very fast and stable fullerene cage based redox processes,[14] are reasonably cheap and abundant, as a result of C_{60} being the thermodynamically most stable form of molecular carbon, and can be made extremely soluble in organic[15] and aqueous[16] solvents with appropriate modification. It is therefore remarkable that they have never been explored as candidates for the redox species in RFBs previously. Fullerene derivatives decorated with suitable electron-donating groups can form a species with at least three oxidation states which are separated by more than 1 V, so that one molecule can serve as both anolyte and catholyte and crossover does not chemically contaminate the electrolytes (see Figure 1).
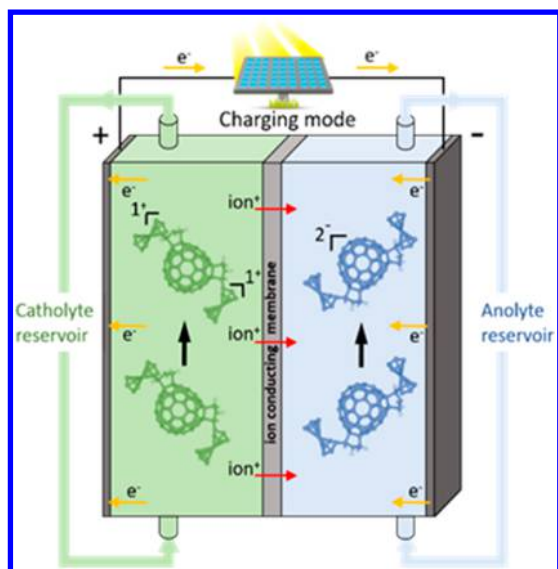
Figure 1. Schematic of the all fullerene RFB setup.

■ RESULTS AND DISCUSSION

Herein, we explore the unique concept of an all-fullerene-based cell, employing an appropriately derivatized fullerene as active species in both catholyte and anolyte as schematically demonstrated in Figure 1. We utilize multiple metallocene moieties appended to the fullerene cage as the catholyte species, while exploiting the inherent, reversible redox processes of the fullerene moiety as the anode-active species. A series of functionalized fullerenes were synthesized containing a number of appended ferrocene units ranging from 1 to 4, **1**–**4**, Figure 2 (see Supporting Information (SI) for full experimental details).
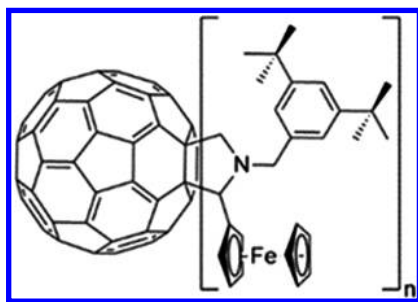

Figure 2. Functionalized fullerene derivatives **1**–**4** ($n = 1$–4).

The fullerene derivatives were observed to be soluble in a variety of solvents and exhibited remarkably high solubility in *ortho*-dichlorobenzene (*O*-DCB) (cf. solubility of **4** in *O*-DCB = 300 ± 22 mg/mL) with a general trend of higher solubility upon addition of more ferrocene moieties (see SI). The redox properties of **1**–**4** were investigated using cyclic voltammetry in *O*-DCB with NBu$_4$BF$_4$ as the supporting electrolyte. All potentials are reported versus Ag$^+$/AgNO$_3$. Figure 3a shows two consecutive one-electron waves associated with reduction and oxidation of the C$_{60}$-cage of **1** at low potentials, $U_0^{C60,1}$ = −0.97 V and $U_0^{C60,2}$ = −1.36 V, and the redox wave for the attached ferrocene at U_0^{Fc} = 0.34 V. This indicates that a single molecule, **1**, transfers two electrons at a potential suitable for an anolyte, and one electron at significantly higher potential. In a battery, potential differences of ΔU^1 = 1.31 V and ΔU^2 =
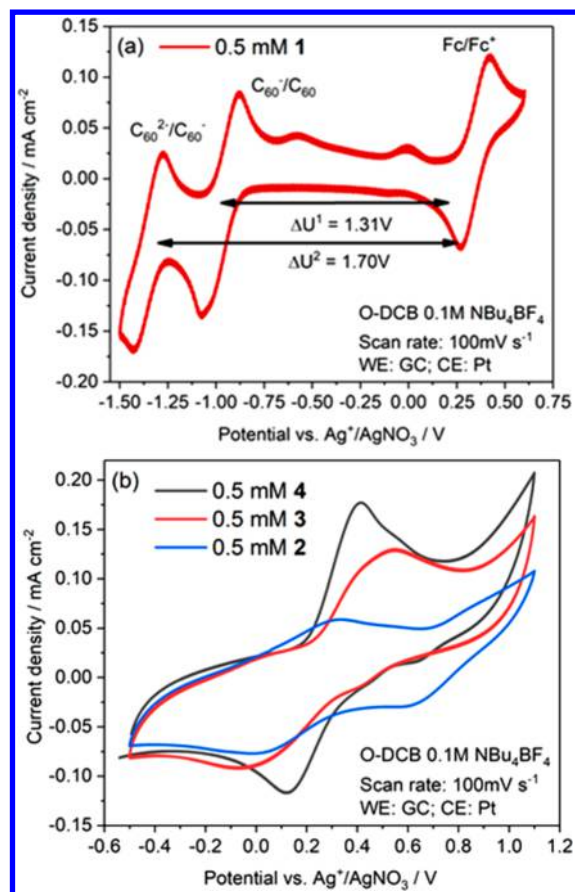

Figure 3. Cyclic voltammograms of (a) **1** and (b) **2**, **3**, and **4** in *O*-DCB with 0.1 M NBu$_4$BF$_4$ as supporting electrolyte.

1.70 V could therefore be established. Employing sampled current voltammetry (SCV) we determined a rate constant for the Fc/Fc$^+$ redox reaction of at least $k_0^{1,Fc}$ = 0.397 cm s^{-1} and a transfer coefficient of α = 0.60 (see Figure S7). This is similar to values of k_0^{Fc} = 1.02 ± 0.009 cm s^{-1} and α = 0.60 ± 0.05 determined for freely diffusing ferrocene/ferrocenium in acetonitrile by SCV on microelectrodes.[17] The kinetics observed are orders of magnitude higher than that for other redox couples employed in RFBs (e.g., VO^{2+}/VO$_2^+$: k_0 = 10^{-6} cm s^{-1}).[18]

The standard potentials of the C$_{60}$ reductions are given in Table S2 and shown in Figure S6. As expected, due to the saturation of double bonds on the molecule, the potentials for the C$_{60}$ reductions shift to more negative values for higher Fc adducts.[19] Good cycling stability was demonstrated for **4**, which showed no change in its electrochemical response when cycled 100 times (see Figure S7). Initial battery studies were performed in a stationary cell optimized for small volumes of electrolyte. Two carbon felt electrodes were soaked in anolyte and catholyte solution respectively and separated by a glass fiber separator. Absorption experiments established that the absorption of fullerene−ferrocene derivatives on the carbon felt is negligible (see Table S6). Preliminary tests were performed to confirm that capacitive processes do not contribute to the measured capacity of fullerene-based cells (Figure S10). A cell with 4 mM ferrocene as the catholyte and 2 mM indene-C$_{60}$ bis-adduct (ICBA), a commercially available fullerene, as the anolyte showed a negligible discharge capacity (Figure S10), indicating that free Fc is not a suitable catholyte,

despite its application as a redox-shuttle in mediated RFBs.[20] This might be due to crossover of the comparatively small Fc molecule through the separator. The fullerene cage of the molecule in the anolyte, ICBA, exhibited redox waves like the C_{60}/C_{60}^- and C_{60}^-/C_{60}^{2-} waves of **1** (compare Figure S9 and Figure 3a).

Four cells were constructed using *O*-DCB and 0.1 M NBu$_4$BF$_4$ to test different fullerene-based cell chemistries. Figure 4a shows a cell utilizing the Fc/Fc$^+$ redox reactions of **2**
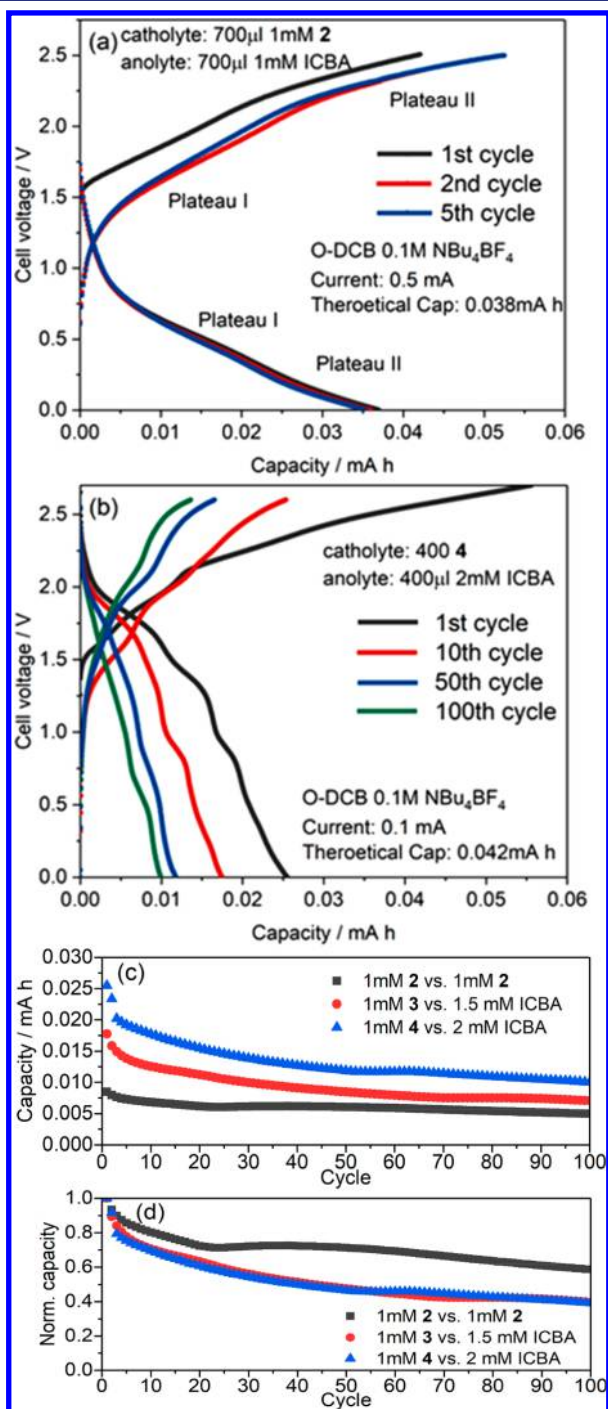

Figure 4. Charge and discharge curves for (a) **2**/ICBA and (b) **4**/ICBA in *O*-DCB with 0.1 M NBu$_4$BF$_4$. Capacity retention plots as (c) discharge capacity versus cycle number and (d) normalized capacity for the investigated systems.

as the catholyte and the C_{60} redox reactions of ICBA as the anolyte. This is referred to as the **2**/ICBA cell and, with 1 mM of two-electron-transferring molecules **2** and ICBA, has a theoretical capacity, Q^{theo}, of 0.038 mA h. This value is almost reached in discharge cycles 1−5 at a current of 0.5 mA. The difference in charging voltage to discharge voltage is high, implying a low voltage efficiency for the **2**/ICBA cell in *O*-DCB. However, the average voltage locations match with the potential positions for the redox reactions shown in Figure 3a, indicating that Plateau I stems from the peaks constituting $\Delta U^1 = 1.31$ V, and Plateau II from those that make up $\Delta U^2 = 1.70$ V. The simple glass fiber separator prevents instantaneous crossover and is therefore an easy and inexpensive solution, working solely on size exclusion which is especially suitable for symmetric systems like **2**/**2**. 100 cycles of charge and discharge were investigated for 1 mM solutions of the more highly derivatized fullerene molecules **3** and **4** versus an appropriate concentration of ICBA to balance the charge of the functionalized C_{60}. These cells are labeled **3**/ICBA (Figure S11) and **4**/ICBA respectively, with the curves for the latter shown in Figure 4b. One more cell, **2**/**2**, with **2** as both as the anolyte and catholyte showcases the concept of a symmetric RFB chemistry with fullerene derivatives (Figure S12). This symmetric chemistry has the advantage that any crossover of redox species through the separator does not lead to a chemical contamination. Rebalancing can be achieved either by mixing the anolyte and catholyte[21] or an added electrolysis cell.[22]

Charge and discharge cycles for the symmetric **2**/**2** cell and the unsymmetrical **3**/ICBA and **4**/ICBA cells are shown in Figure 4c. All three systems look similar, with the charge transferred increasing from **2** to **4**. This is expected, as the concentrations of **2**−**4** were kept constant at 1 mM; therefore, additional Fc groups in molecules with higher degrees of functionalization lead to increased capacity, shown in Figure 4c. Interestingly, the capacity decay for samples **3** and **4** seems to be faster than that for **2**, as shown in Figure 4d which gives the discharge capacity normalized to the charge of the first discharge cycle. There are three explanations for the capacity loss. First, the electrolyte soaks into the dry separator, leading to a loss in active species within the electrode. Second, permeation of anolyte into the catholyte half-cell and vice versa. Third, decomposition of the redox molecules. Importantly, the shapes of all curves do not change over 100 cycles, and HPLC and mass spectrometry of the solutions after 100 cycles confirm that the molecules remain intact. However, an additional, unknown species is also observed to be formed which requires further investigations; see SI for full details. Most likely, all three mechanisms play a role. We hypothesize that soaking of the separator leads to the initial capacity loss in the first few cycles, as the fade is similar for all three cells (Figure 4d). Subsequent loss could be due to crossover and decomposition. As crossover is less of an issue for the **2**/**2** cell, its higher capacity retention than **3**/ICBA and **4**/ICBA can be rationalized.

While the three-electrode measurements and also the charge−discharge behavior look promising, the low voltage efficiency shown in Figure 4 is a problem. The cell voltage U depends on the current I:[1]

$$U(I) = \Delta U \pm I \cdot R_{CT} \pm I \cdot R_{Diff} \pm I \cdot R_{Ohm} \qquad (1)$$

with potential difference between the two half-cells, ΔU; charge transfer resistance for all redox processes, R_{CT}; mass

transport resistance, R_{diff}; and the sum of all ohmic losses, R_{ohm}. The plus sign is applicable for the charging process, and the minus sign, for the discharge. Because R_{CT} is inversely proportional to k_0 and therefore small, and R_{Diff} is small because in our stationary cell all electrolyte is within the porous electrode, the overvoltage must stem from R_{Ohm}. R_{Ohm} comprises the resistance of the electrolyte and of the separator. This can be understood because in this configuration the bulky tetrabutylammonium cation is required to cross the separator to balance the charge. Electrochemical impedance spectroscopy (ESI) measurements showed a significantly lower R_{Ohm} for DMF with 0.1 M LiCl (7 Ω) in the stationary cell than for O-DCB with 0.1 M NBu$_4$BF$_4$ (211 Ω) or 1.0 M NBu$_4$BF$_4$ (42 Ω) as shown in Figure S15. Thus, cells with DMF as solvent and 0.1 M LiCl as electrolyte were tested. To avoid the contribution of water and oxygen, the cell assembly process and the preparation of the electrolytes were performed in a glovebox and an airtight cell was used.

The **4**/ICBA cell in DMF with 0.1 M LiCl was cycled 100 times at 1 mA revealing a current 10 times higher than that for a similar cell in O-DCB (Figure S13b). However, in DMF the shapes of the charge−discharge curves do not remain stable. As can be seen in Figure S13a, the higher discharge plateau gradually vanishes, and the lower plateau is then providing the capacity. These findings are supported by post-mortem HPLC and mass spectroscopy studies that found ICBA, but only traces of **4** after 100 cycles. The exact decomposition mechanism of **4** is unclear and requires further investigation. It is unlikely to be due to the retro-Prato reaction,[23] as we do not observe formation of lower Fc adducts or unfunctionalized fullerene. Interestingly the capacity of cell **4**/ICBA remains relatively stable throughout (Figure S13b).

The cell chemistry shown in Figure S13 is able to produce a discharge current of 10 mA at a concentration of 1 mM. The electrode material was a GFD felt with surface area 1 cm^2 and thickness 4.6 mm. This shows that fullerene-based chemistry could enable high power RFBs. Current VRBs exhibit a current density of 0.07 A cm^{-2}.[24] Using the measured concentration of **4** (0.12 M), and assuming that the current scales with concentration, a current density of 1.2 A cm^{-2} could be drawn from such a cell. Figure S14 shows the rate capability of the **4**/ICBA cell. A comparison of how this and other metrics relate to other reported RFB chemistries is shown in Table 1.

Being composed entirely of abundant, sustainable elements, our electrolyte system should face minimal resistance to scale-up, and thus we estimate bulk chemical costs of $15 and $11 kW h^{-1} for the **4**/ICBA and **2**/**2** electrolytes respectively based on raw materials.[3] These costs can be compared directly with reported values of $7−21 kW h^{-1} for bromine and AQDS systems and $83 kW h^{-1} for vanadium flow batteries (see SI for information on cost calculations).[3] However, clearly such approximations do not give the full picture and costs such as the supporting electrolyte, which are currently unworkably high (cf. NBu$_4$BF$_4$ costs ∼$12 500 kW h^{-1}) and need to be reduced, by using either cheaper salts or conductive solvents such as ionic liquid, for nonaqueous RFB systems to be competitive.[25] In summary, we have made a series of highly soluble redox active fullerene−ferrocene derivatives and fully characterized their electrochemical behavior revealing multiple fast and reversible redox processes. We have explored their potential as multiple charge shuttles for redox flow batteries in two electrolytes. In O-DCB with 0.1 M NBu$_4$BF$_4$ we have observed high solubility (exceptionally high for fullerene

Table 1. Performance Metrics of the Presented Chemistries and Literature Studies

Cell[a]	Solvent/electrolyte	OCV (V)	Current density per concn (mA cm^{-2} mol^{-1})	Energy density per concn (W h mol^{-1} L)
4/ICBA	O-DCB/0.1 M NBu$_4$BF$_4$	1.49	500	80
2/**2**	O-DCB/0.1 M NBu$_4$BF$_4$	1.64	500	44
4/ICBA	DMF/0.1 M LiCl	1.49	10 000	80
VRB[2]	Water/2 M H$_2$SO$_4$	1.26	44	17
AQDS/Br[3]	Water/1 M H$_2$SO$_4$	0.81	500	22
TEMPO/VIOL[6]	Water/1 M NaCl	1.1	267	15
NMP/benzene deriv.[9]	DME/1 M LiTFSI	2.3	167	31

[a]See the SI for an explanation of the values and the performed calculations.

derivatives), increasing capacity with increasing number of ferrocene adducts and charge−discharge curves that do not alter their shape over 100 cycles. However, the conductivity of the solvent and supporting electrolyte was low, limiting the charging current to 0.1 mA. We have also demonstrated a symmetric cell, utilizing **2** as anolyte and catholyte. As crossover is less detrimental in a symmetric cell than in an asymmetric cell, this configuration can potentially enable a membrane-free design.[26] A membrane-free design eliminates the ohmic loss of the membrane, and therefore higher current densities than with a separator could be achieved.

In DMF with 0.1 M LiCl, the stability of the Fc-modified fullerenes seems to be limited. During 100 charge and discharge cycles, the shape of the curves changed significantly. Also, post-mortem analysis could detect mostly the ICBA, but only traces of Fc-functionalized fullerene. On the other hand, high current rates up to 10 mA gave reasonable efficiencies. We can exclude that the Fc-functionalized fullerenes simply decompose and the Fc is active in solution, as cells with 4 mM Fc in DMF and 0.1 M LiCl showed a negligible discharge capacity (Figure S10).

■ CONCLUSION

The current system demonstrates a novel concept in terms of redox electrochemistry for RFBs. Two electrolyte systems were investigated both exhibiting some limitations: stability in DMF and rate performance in O-DCB. However, intrinsically both the Fc/Fc$^+$ and the C$_{60}$ redox reactions are facile; the molecules consist only of the cheapest, most abundant elements, i.e. C, N, Fe, and functionalization methods have been developed to enhance fullerene solubility. Therefore, with further work, fullerene-based cells have the potential to revolutionize RFBs by simultaneously increasing the current and energy densities while enabling affordable and sustainable scale up.

■ ASSOCIATED CONTENT

ⓢ Supporting Information

The Supporting Information is available free of charge on the ACS Publications website at DOI: 10.1021/jacs.7b11041.

Details of fullerene synthesis and characterization, solubility, degradation and electrochemistry studies, and RFB performance and costing calculations (PDF)

■ AUTHOR INFORMATION

Corresponding Authors
*t.w.chamberlain@leeds.ac.uk
*ulrich.stimming@ncl.ac.uk
ORCID
Thomas W. Chamberlain: 0000-0001-8100-6452
Notes
The authors declare no competing financial interest.

■ ACKNOWLEDGMENTS

■ REFERENCES

(1) Arenas, L. F.; Ponce de León, C.; Walsh, F. C. *Journal of Energy Storage* **2017**, *11*, 119−153.

(2) Weber, A. Z.; Mench, M. M.; Meyers, J. P.; Ross, P. N.; Gostick, J. T.; Liu, Q. *J. Appl. Electrochem.* **2011**, *41*, 1137−1164.

(3) Huskinson, B.; Marshak, M. P.; Suh, C.; Er, S.; Gerhardt, M. R.; Galvin, C. J.; Chen, X.; Aspuru-Guzik, A.; Gordon, R. G.; Aziz, M. J. *Nature* **2014**, *505*, 195−8.

(4) Lin, K.; Chen, Q.; Gerhardt, M. R.; Tong, L.; Kim, S. B.; Eisenach, L.; Valle, A. W.; Hardee, D.; Gordon, R. G.; Aziz, M. J.; Marshak, M. P. *Science* **2015**, *349*, 1529−1532.

(5) Beh, E. S.; De Porcellinis, D.; Gracia, R. L.; Xia, K. T.; Gordon, R. G.; Aziz, M. J. *ACS Energy Lett.* **2017**, *2*, 639−644.

(6) Janoschka, T.; Martin, N.; Martin, U.; Friebe, C.; Morgenstern, S.; Hiller, H.; Hager, M. D.; Schubert, U. S. *Nature* **2015**, *527*, 78−81.

(7) Milshtein, J. D.; Kaur, A. P.; Casselman, M. D.; Kowalski, J. A.; Modekrutti, S.; Zhang, P. L.; Harsha Attanayake, N.; Elliott, C. F.; Parkin, S. R.; Risko, C.; Brushett, F. R.; Odom, S. A. *Energy Environ. Sci.* **2016**, *9*, 3531−3543.

(8) Duan, W.; Huang, J.; Kowalski, J. A.; Shkrob, I. A.; Vijayakumar, M.; Walter, E.; Pan, B.; Yang, Z.; Milshtein, J. D.; Li, B. *ACS Energy Lett.* **2017**, *2*, 1156−1161.

(9) Wei, X.; Duan, W.; Huang, J.; Zhang, L.; Li, B.; Reed, D.; Xu, W.; Sprenkle, V.; Wang, W. *ACS Energy Lett.* **2016**, *1*, 705−711.

(10) Wei, X.; Xu, W.; Huang, J.; Zhang, L.; Walter, E.; Lawrence, C.; Vijayakumar, M.; Henderson, W. A.; Liu, T.; Cosimbescu, L.; Li, B.; Sprenkle, V.; Wang, W. *Angew. Chem., Int. Ed.* **2015**, *54*, 8684−8687.

(11) Winsberg, J.; Hagemann, T.; Janoschka, T.; Hager, M. D.; Schubert, U. S. *Angew. Chem., Int. Ed.* **2017**, *56*, 686−711.

(12) Leung, P.; Shah, A. A.; Sanz, L.; Flox, C.; Morante, J. R.; Xu, Q.; Mohamed, M. R.; Ponce de León, C.; Walsh, F. C. *J. Power Sources* **2017**, *360*, 243−283.

(13) Noack, J.; Roznyatovskaya, N.; Herr, T.; Fischer, P. *Angew. Chem., Int. Ed.* **2015**, *54*, 9776−9809.

(14) Echegoyen, L.; Echegoyen, L. E. *Acc. Chem. Res.* **1998**, *31*, 593−601.

(15) Ganesamoorthy, R.; Sathiyan, G.; Sakthivel, P. *Sol. Energy Mater. Sol. Cells* **2017**, *161*, 102−148.

(16) Yamakoshi, Y.; Aroua, S.; Nguyen, T.-M. D.; Iwamoto, Y.; Ohnishi, T. *Faraday Discuss.* **2014**, *173*, 287−296.

(17) Birkin, P. R.; Silva-Martinez, S. *Anal. Chem.* **1997**, *69*, 2055−62.

(18) Friedl, J.; Stimming, U. *Electrochim. Acta* **2017**, *227*, 235−245.

(19) Carano, M.; Da Ros, T.; Fanti, M.; Kordatos, K.; Marcaccio, M.; Paolucci, F.; Prato, M.; Roffia, S.; Zerbetto, F. *J. Am. Chem. Soc.* **2003**, *125* (23), 7139−7144.

(20) Huang, Q.; Li, H.; Grätzel, M.; Wang, Q. *Phys. Chem. Chem. Phys.* **2013**, *15*, 1793−7.

(21) Tang, A.; Bao, J.; Skyllas-Kazacos, M. *J. Power Sources* **2011**, *196*, 10737−10747.

(22) Rudolph, S.; Schröder, U.; Bayanov, I. M. *J. Electroanal. Chem.* **2013**, *703*, 29−37.

(23) Martín, N.; Altable, M.; Filippone, S.; Martín-Domenech, A.; Echegoyen, L.; Cardona, C. M. *Angew. Chem., Int. Ed.* **2006**, *45*, 110−114.

(24) Zhao, P.; Zhang, H.; Zhou, H.; Chen, J.; Gao, S.; Yi, B. *J. Power Sources* **2006**, *162*, 1416−1420.

(25) Dmello, R.; Milshtein, J. D.; Brushett, F. R.; Smith, K. C. *J. Power Sources* **2016**, *330*, 261−272.

(26) Navalpotro, P.; Palma, J.; Anderson, M.; Marcilla, R. *Angew. Chem., Int. Ed.* **2017**, *56*, 12460−12465.